IRINA

Проект ИРИНА: Лазерная (ядерная) спектроскопия на реакторе ПИК

IRINA: Yields

Yields were calculated with 5 g of ^{235}U in target and $3×10^{13}$ n/cm^2/s

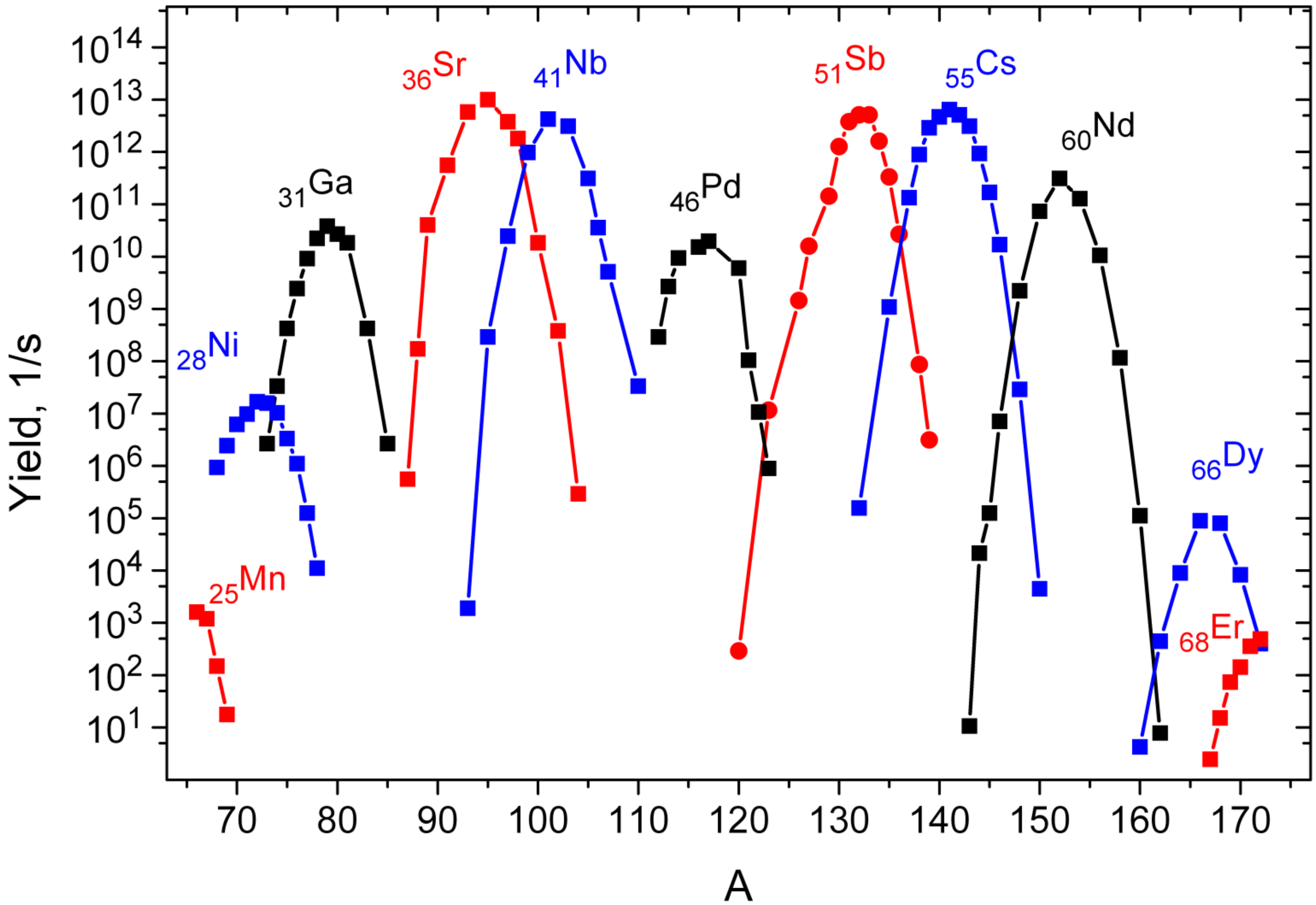

IRINA: r-process

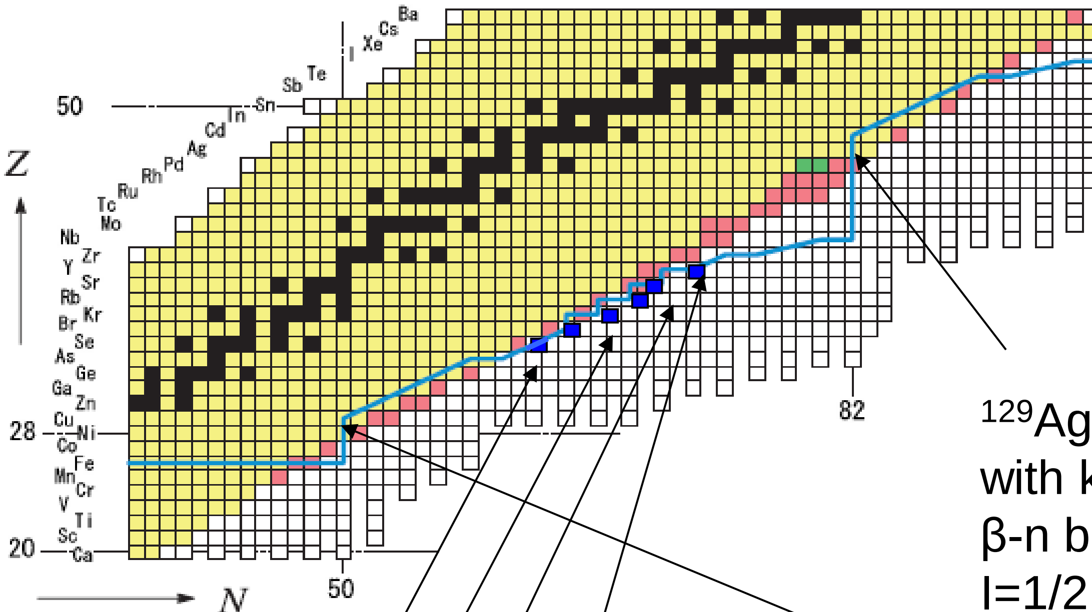

^{95}Se ~ 10^2, ^{98}Br ~ 10^3, ^{101}Kr ~ 10^4, ^{103}Rb ~ 10^5 (RIKEN-RIBF ~ 50), ^{106}Sr ~ 10^3, ^{109}Y ~ 10^3

^{129}Ag, ^{78}Ni : waiting points with known $T_{1/2}$ and unknown β-n branchings. $T_{1/2}$ for ^{129}Ag I=1/2 isomer and its excitation energy are not known. Expected yields ^{129}Ag ~ 1 1/s; ^{78}Ni ~ 10^4 1/s

(RIKEN: ^{238}U+Be, 345 MeV/n, 6×10^{10} 1/s — 10^4 ^{78}Ni in 13 days)

T. Ohnishi et al., Phys. Soc. Jap. 79, 2010, 073201

IRINA: r-process

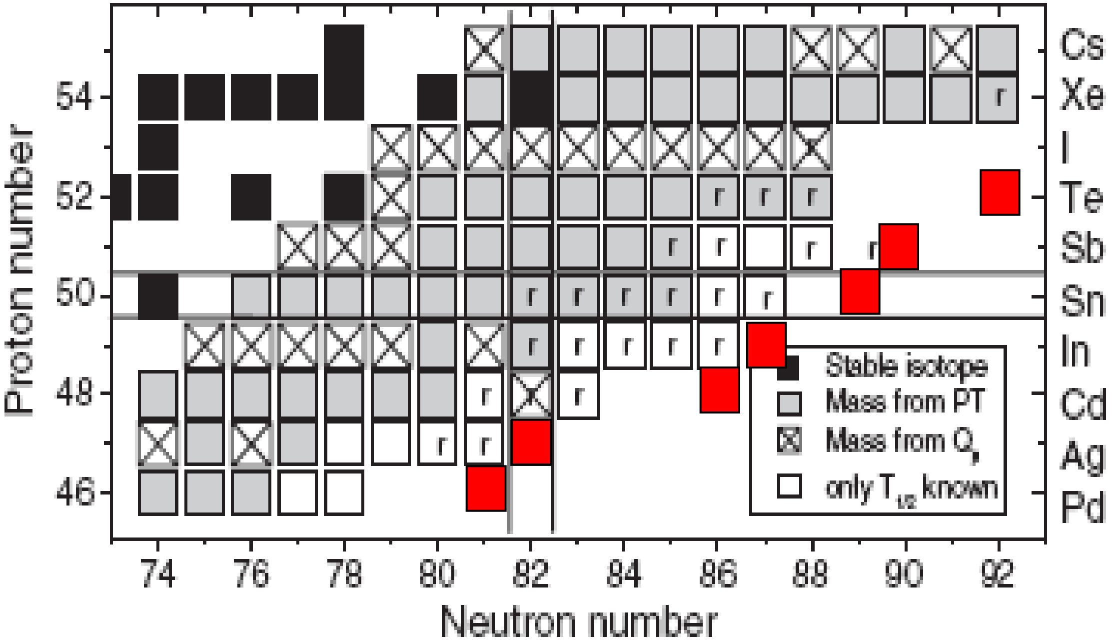

Last accessible at IRINA

J. Hakala et al., Phys. Rev. Lett. 109, 032501 (2012)

Shell evolution for exotic nuclei

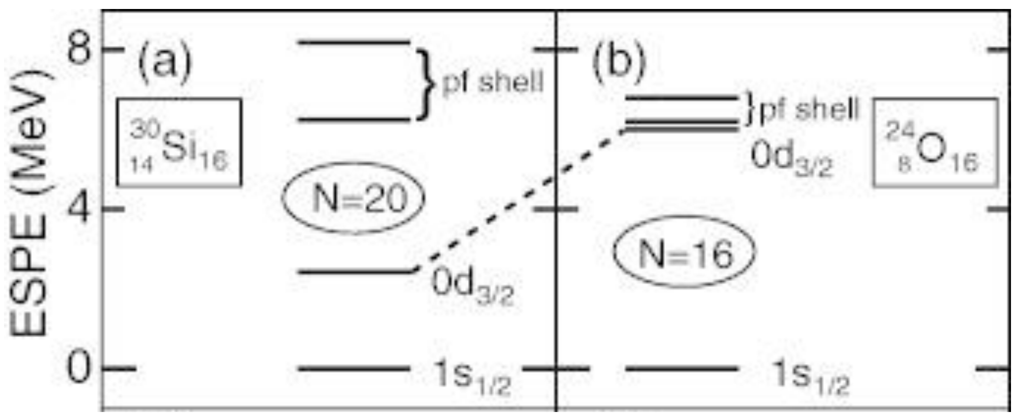

Neutron single particle energies for (a) ^{30}Si and (b) ^{24}O, relative to $1s_{1/2}$.

Shell evolution:
^{24}O — new magic number at N=16,
^{54}Ca — new magic number at N=34,
disappearance of the N=20 (^{32}Mg) and 28 (^{42}Si) shell gaps, etc.
It was explained by introducing ***tensor forces*** or/and ***3N forces***

For O the drip line is strikingly close to the stability line (last bound is doubly magic ^{24}O; cf. last bound ^{31}F, Z=8+1).
This phenomenon was explained by introducing ***3N forces***.
(See EFT studies with naturally arisen 3N forces: E. Epelbaum et al., RMPh, 81 (2009) 1773)

T. Otsuka Phys. Scr. (2013) 014007

Disappearance of N=40 sub-shell

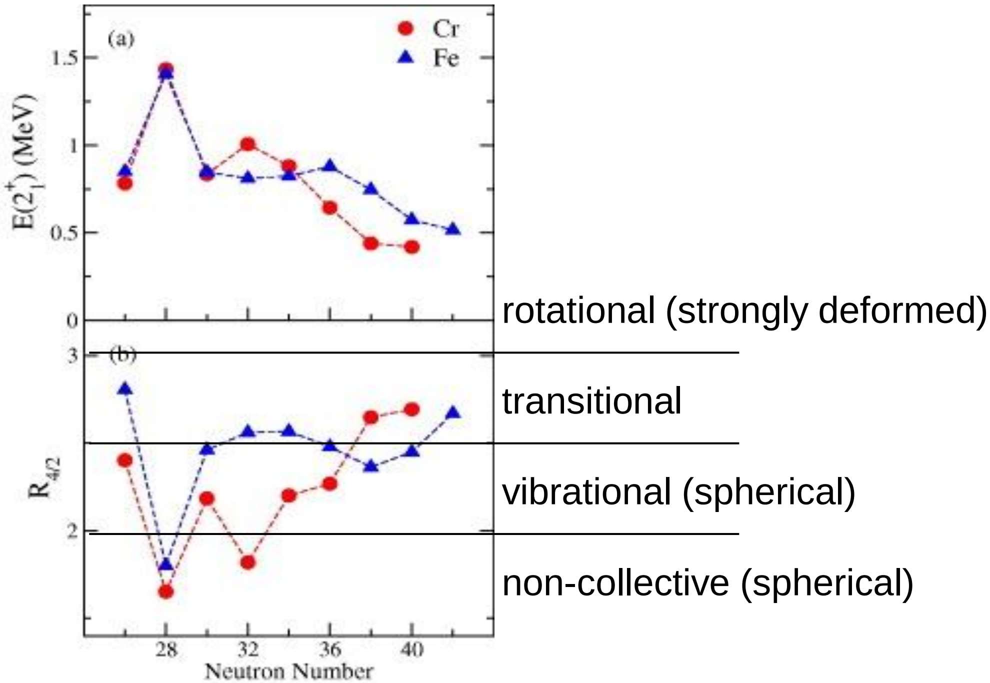

$E(2^+)$ and $R(E_{4+}/E_{2+})$ systematics for neutron-rich $_{24}$Cr and $_{26}$Fe isotopes in the range 26 ≤ N ≤ 40.

The different behavior of excitation energies for these Cr and Fe isotopes point to a different intrinsic structure for the two N = 40 isotones. These observations represent a challenge for the most modern nuclear interactions.

R. V. F. Janssens, Phys. Scr. (2013) 014005

IRINA: disappearance of N=40 shell

Calculations: ground states of all the Fe isotopes are predominantly of spherical character, whereas ground states of $^{62,64}Cr$ are dominated by a deformed configurations.

Striking similarity with Pb region: shape coexistence predicted.

$^{67}Co^{40}$ ~ 4.5×10^{5} 1/s

$^{65}Mn^{40}$ ~ 10^{4} 1/s

$^{69}Mn^{44}$ ~ 20 1/s

$^{64}Cr^{40}$ ~ 10÷100 1/s

$^{66}Fe^{40}$ ~ 8×10^{4} 1/s

$^{73}Fe^{47}$ ~ 10 1/s

Previously measured		Achievable at IRINA
$^{54-58}Fe^{28-32}$	⇨	up to N=46
$^{50-56}Mn^{25-31}$	⇨	up to N=44
$^{50-54}Cr^{26-30}$	⇨	up to N=40

Shell-effect in radii at N=126, Z=82

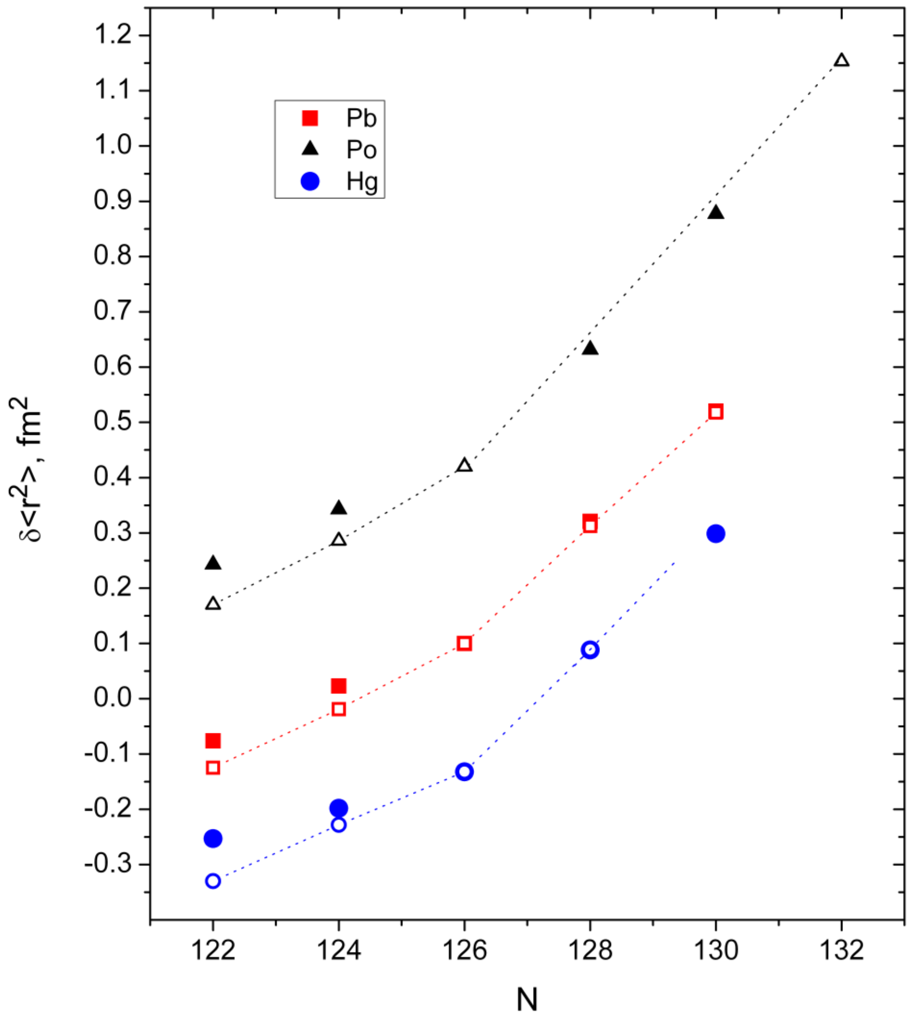

Hollow symbols — experiment

Full symbols — RMF calculations

(σ scalar, isoscalar
ρ vector, isovectot
ω vector, isoscalar)

G. A. Lalazissis et al., ADNDT 71, 1 (1999)

P. M. Goddard et al., PRL, **110**, 032503, 2013.

IRINA: shell-effect in radii at N=82, Z=50

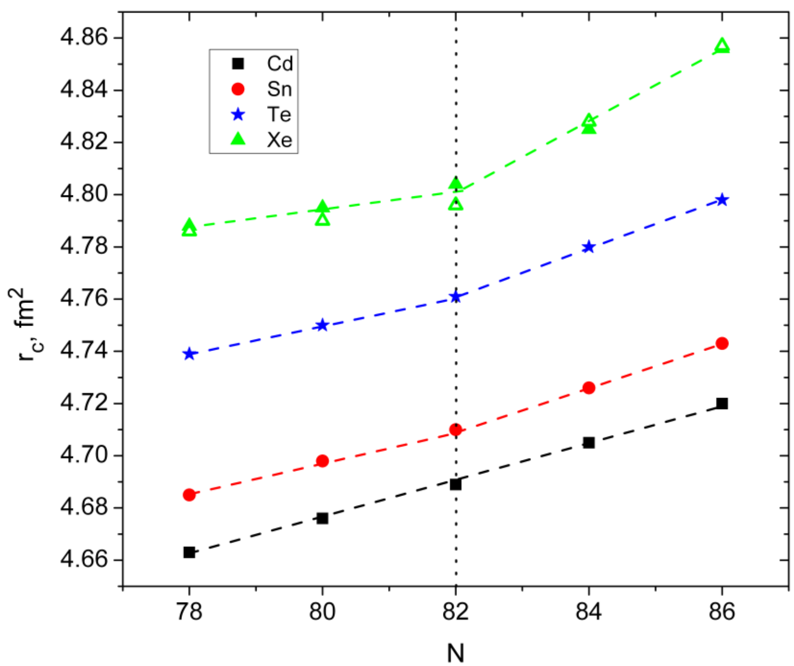

theory (RMF)

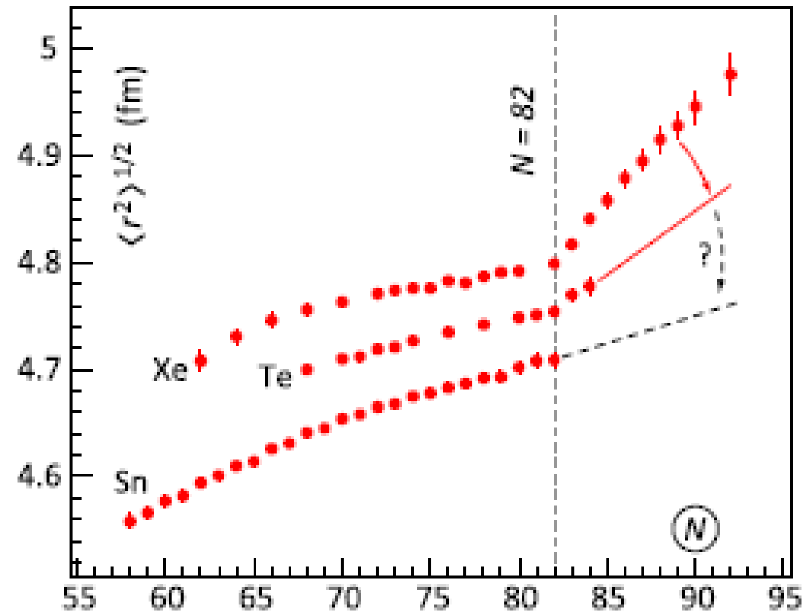

experiment

G. A. Lalazissis et al., ADNDT 71, 1 (1999)

Previously measured		Achievable at IRINA
$^{102-129}Cd^{54-81}$	⇒	up to N=86
$^{104-127}In^{55-78}$	⇒	up to N=87
$^{108-132}Sn^{58-82}$	⇒	up to N=89
(Sb)	⇒	N=69-90
$^{120-136}Te^{68-84}$	⇒	up to N=92

N>88 — classical deformation region!

New shell closure at N=90, Z~50 is predicted.

Shell-effect in radii at N=50

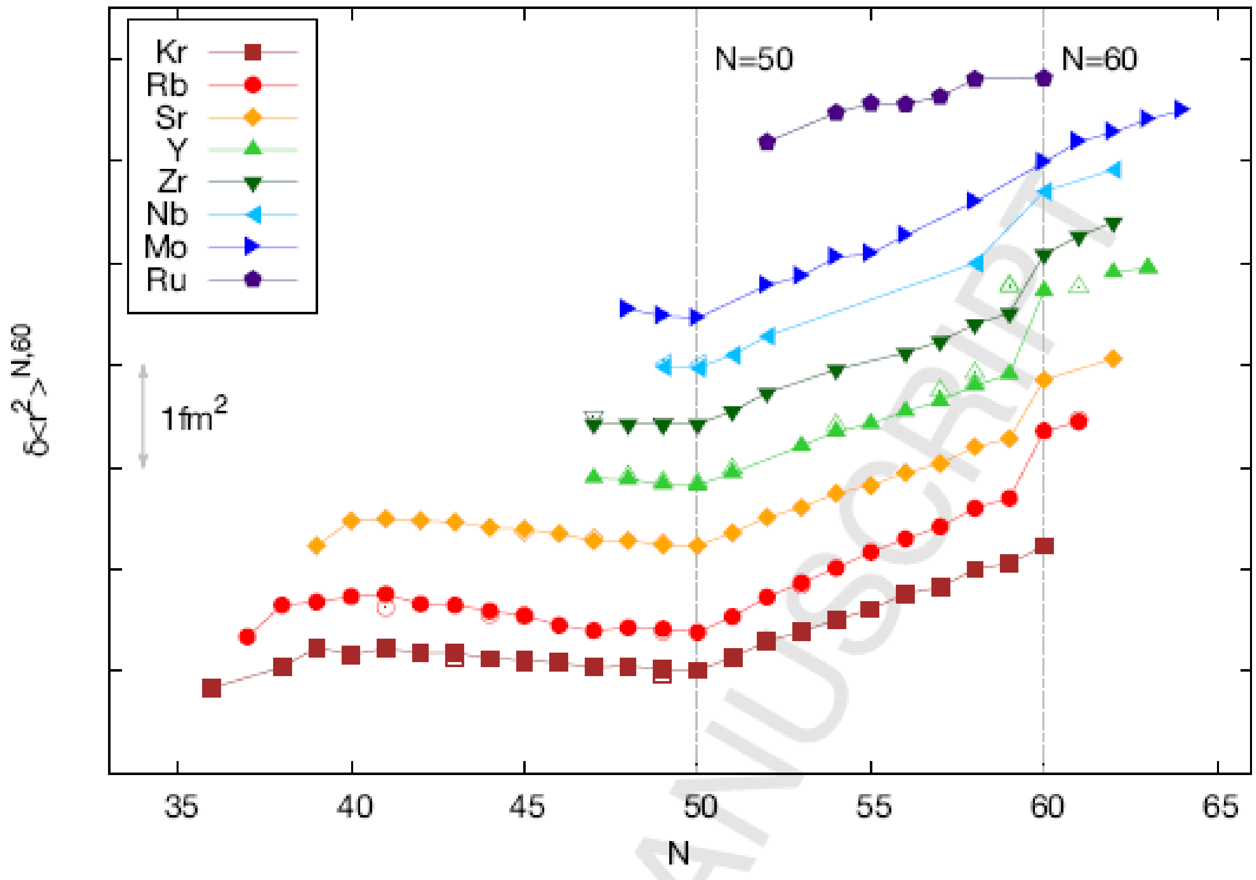

The same kink in Ga (very n-rich)

P. Campbell et al., Progress in Particle and Nuclear Physics (2015)

IRINA: shell-effect in radii at N=50, Z=28

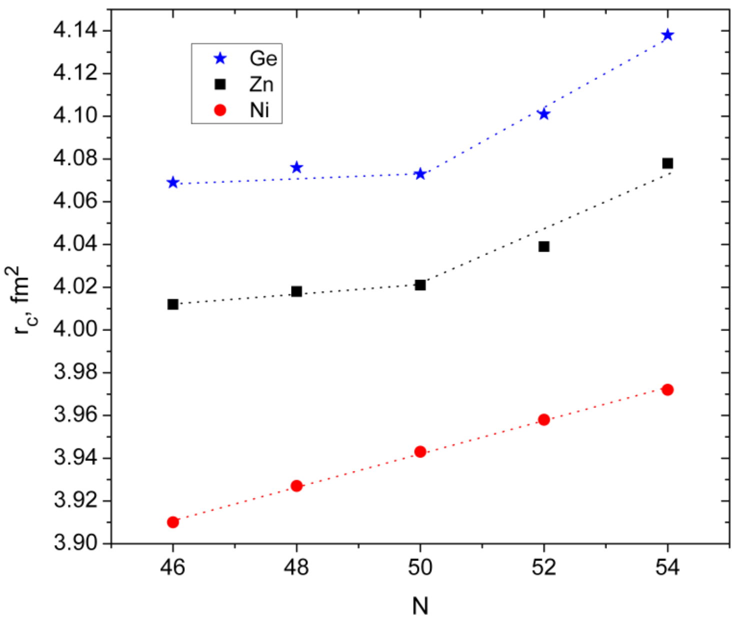

theory (RMF)

G. A. Lalazissis et al., ADNDT 71, 1 (1999)

Achievable at IRINA

$_{28}$Ni up to N=52

$_{30}$Zn up to N=56

$_{32}$Ge up to N=57

Previously measured: $^{63\text{-}82}Ga^{32\text{-}51}$ → Achievable at IRINA: up to N=56

Shell evolution for exotic nuclei

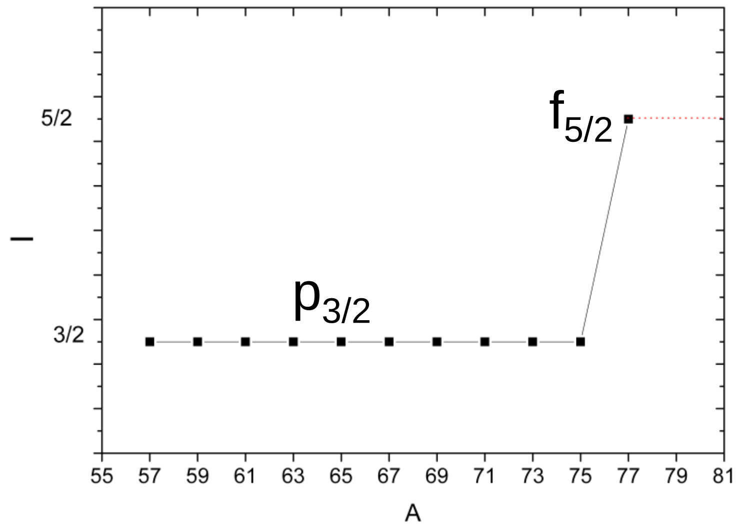

spins for odd $_{29}$Cu isotopes

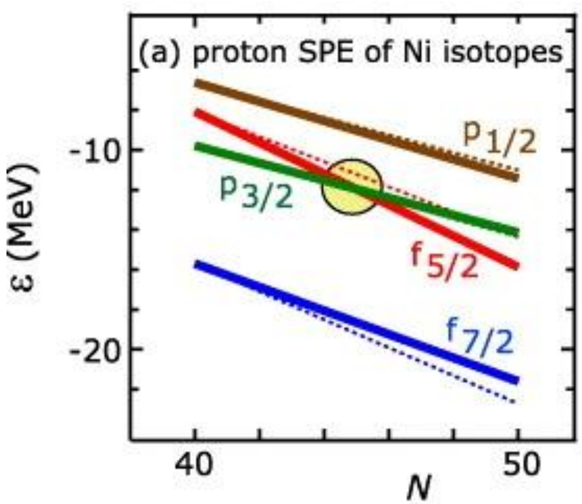

SPEs of protons for Ni isotopes

$f_{5/2}$ / $p_{3/2}$ inversion was shown by I and μ laser measurements (^{71,73,75}Cu) and may be explained with ***tensor force*** inclusion. (See also shell quenching)

It is of importance to trace the proton shell evolution beyond N=50.

Same inversion was found for Ga (A=79-81, N=48-50).

T. Otsuka Phys. Scr. (2013) 014007

Shell evolution for exotic nuclei

K. T. Flanagan et al., PRL 103, 142501 (2009)

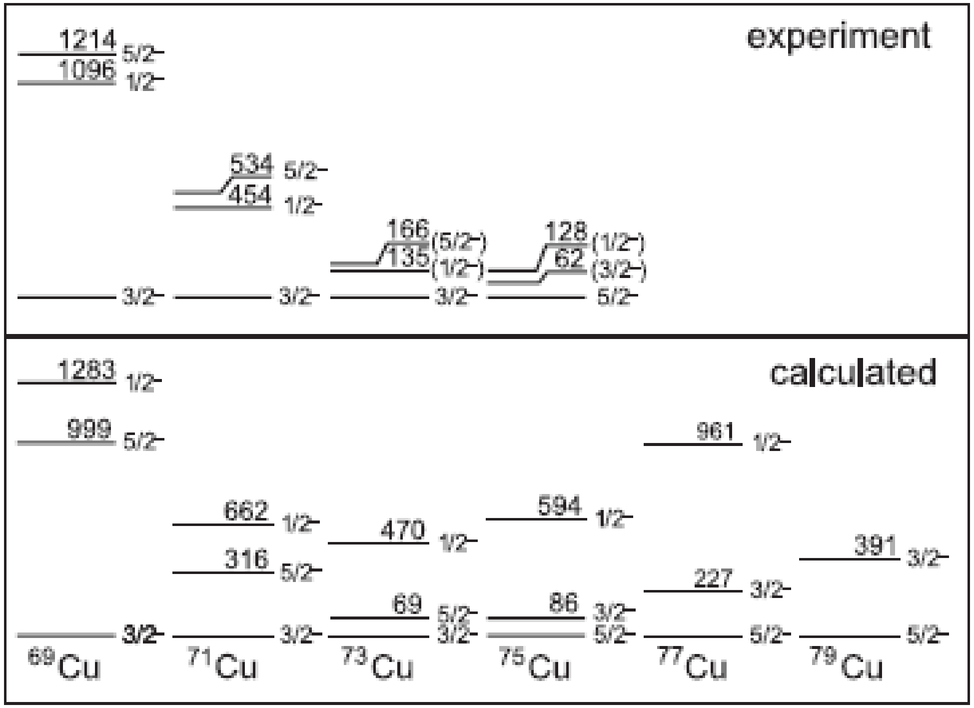

Lowering of $p_{1/2}$ state was reproduced only after Z=28 shell quenching taking into account

K. Sieja and F. Nowacki, Phys. Rev. C **81**, 061303 (2010)

Shell evolution for exotic nuclei

K. T. Flanagan et al., PRL 103, 142501 (2009); U. Köster et al., PRC **84**, 034320 (2011)

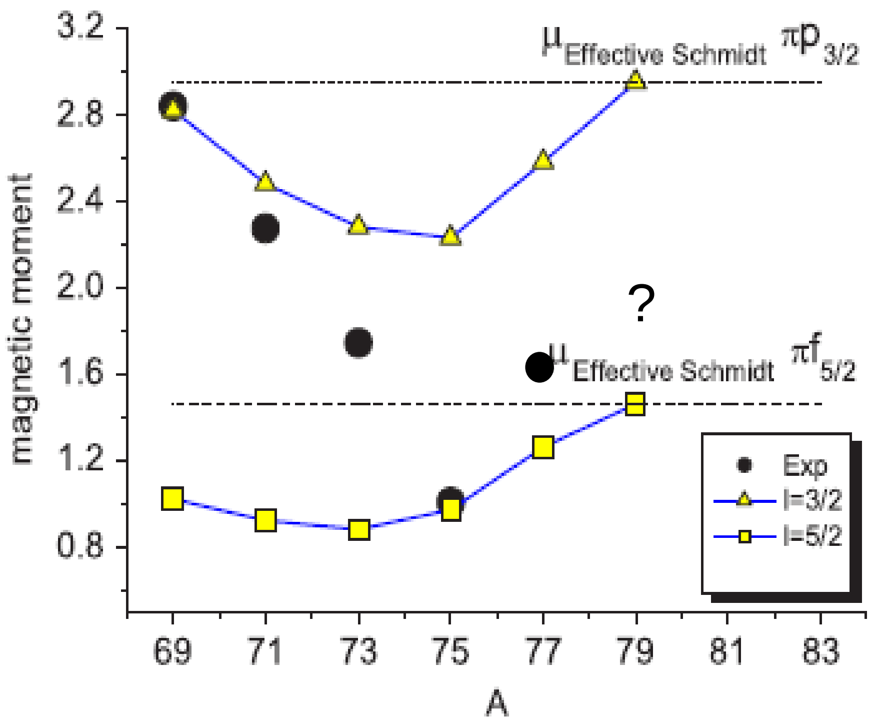

Unexplained lowering of $p_{1/2}$ state is responsible for the discrepancy between theory and experiment for μ(^{71,73}Cu)

Disagreement for μ(^{77}Cu)?

IRINA: Shell evolution for exotic nuclei

K. Sieja and F. Nowacki, Phys. Rev. C **81**, 061303 (2010).

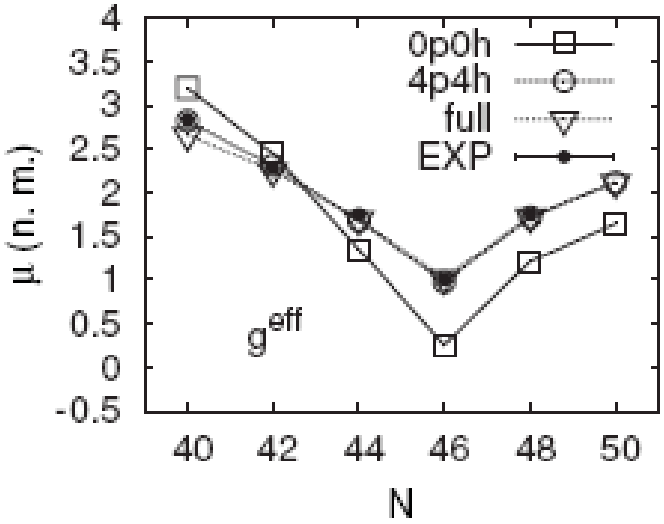

μ(^{77}Cu) may be reproduced only with Z=28 shell quenching by 0.7MeV

Previously measured		Achievable at IRINA
$^{57-78}Cu^{29-49}$	⇒	up to N=53
$^{63-82}Ga^{32-51}$	⇒	up to N=56

Note: rapid onset of deformation is expected beyond N=50; $T_{1/2}$ for ^{86,87}Ga are needed for r-process studies (shell quenching)

Whether the similar inversion occurs for Z=50 shell? Some indications of "tensor force induced" shell evolution was found in $^{126}Pd^{80}$: small difference between the 10^+ and 7^- isomers was ascribed to the tensor force shift of the $1h_{11/2}$ neutron orbit (H. Watanabe *et al*, PRL 113, 042502 (2014)). See also: J. Shergur et al., Eur. Phys. J. A 25, 121 (2005) ($5/2^+$ state in ^{135}Sb)

Quenching of the N=82 shell gap?

I. Dillmann et al., PRL 91, 162503 (2003)

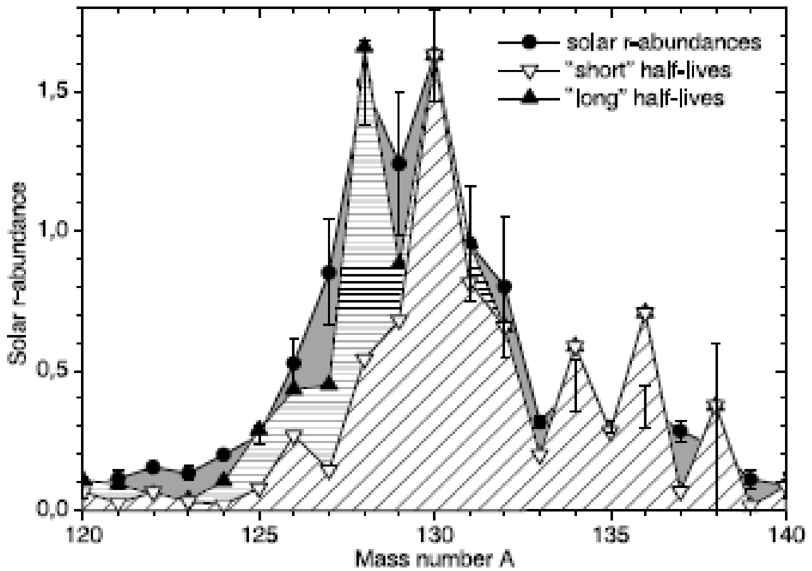

Comparison of the solar system *r*-process abundances in the *A*~130 peak region with model predictions

Quenching of N=82 shell describes big $Q_\beta(^{130}Cd)$, high energy of 1^+ state in ^{130}In and corresponding log(ft). Cf. also improvement of solar r-abundances at A=130 descriptions

$[\pi g_{9/2}, \ \nu g_{7/2}]$ 2QP 1^+ state

$^{129\text{-}132}Cd$, ^{128}Pd, ^{122}Zr masses as well as the position and log(ft) values for 1^+ GT states in daughter nuclei are needed.

$T_{1/2}$ for waiting point ^{128}Pd — 3 1/s at IRINA

IRINA: Reducing pairing after N=82?

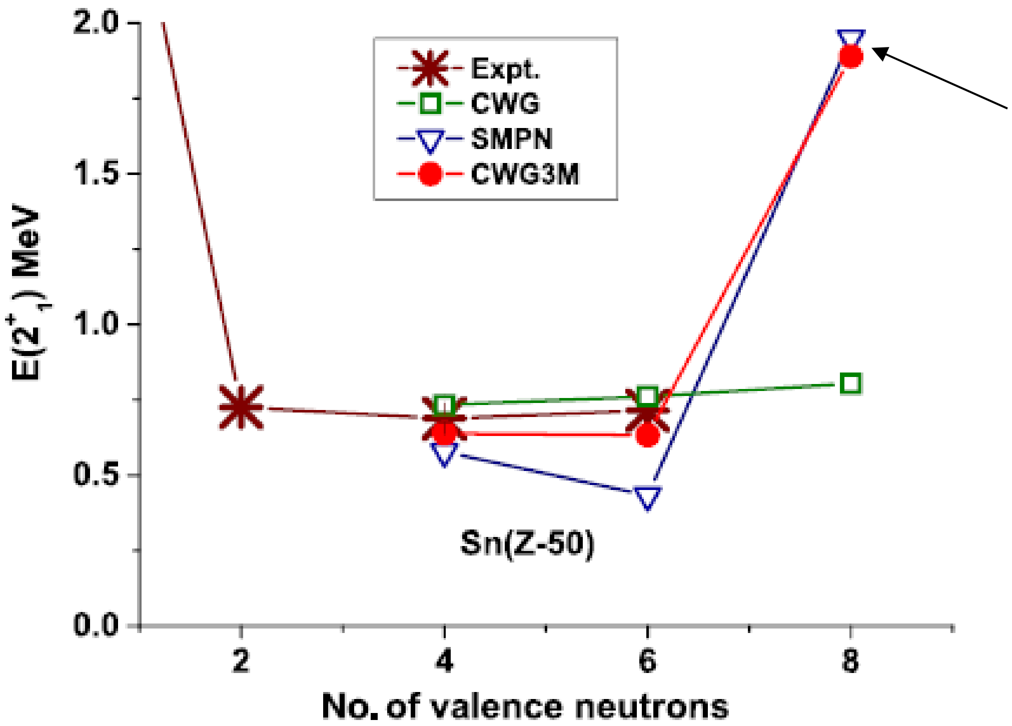

New magic number N=90?
Calculations with 3N forces

$^{136}Te^{84}$ puzzle: decrease of $E(2^+)$ without increase of B(E2) — is described by decrease of pairing after N=82 caused by 3N forces

Description of $E(2^+)$ and B(E2; $6^+ \rightarrow 4^+$) for $^{136,138}Sn$ is better with 3N forces. Crucial will be the measurement of B(E2; $2^+ \rightarrow 0^+$) for ^{136}Sn. Predictions: 184 fm^4 without 3N forces, 73 fm^4 with 3N forces

^{136}Sn at IRINA: 10^6 1/s — RIB is necessary (for B(E2))!

M. Saha Sarkar, and S. Sarkar, Pramana 85 (2015) 403-413

IRINA: Sb isotopic chain

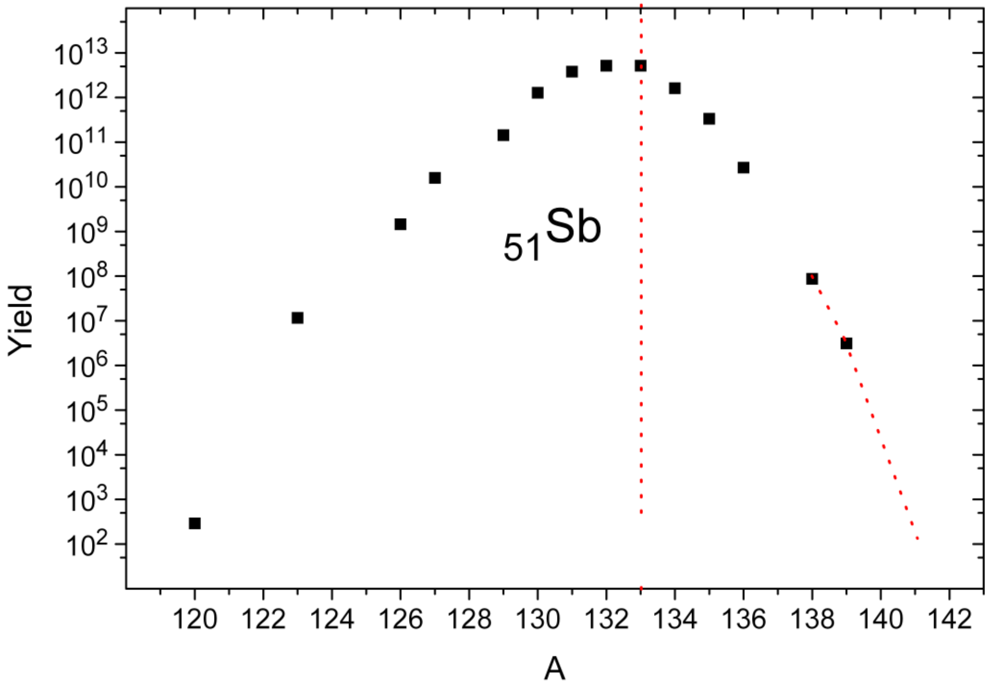

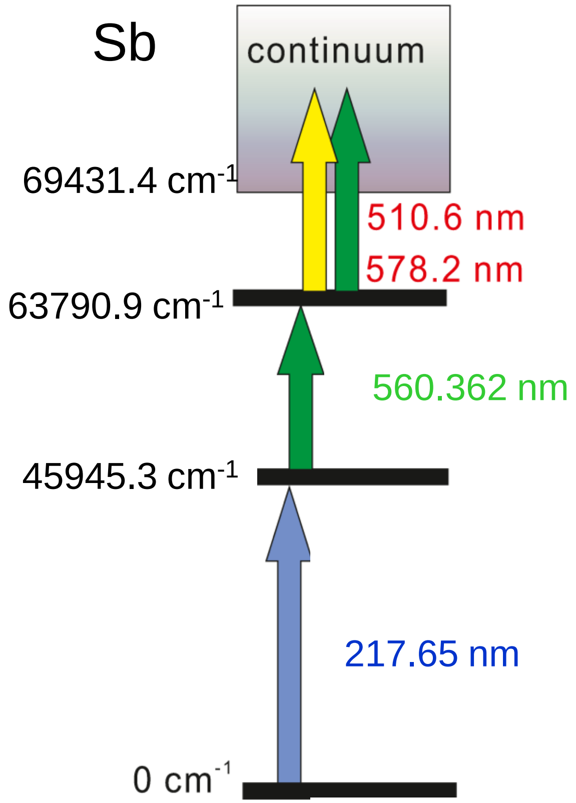

Single particle states near N=82, new N=90 magic number (?), shell effect at N=82…

At IRIS with 1-GeV protons $^{111\text{-}135}$Sb can be measured.

At IRINA this chain can be continued up to A=141.

IRINA: Sb isotopic chain

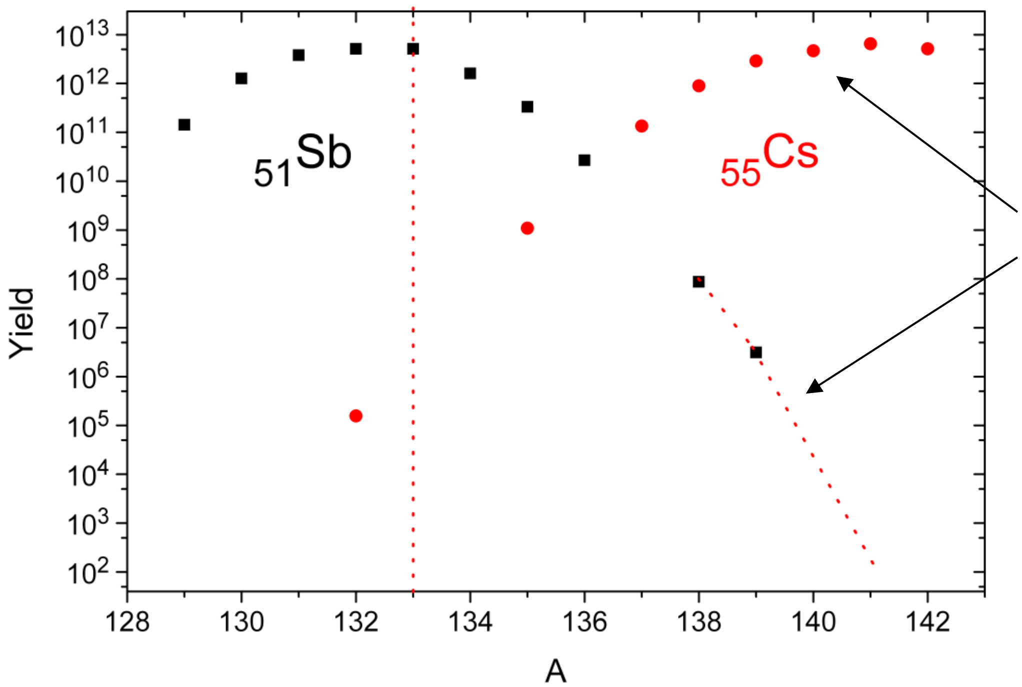

Cs background is 6 orders of magnitude greater than Sb yield!

At A>136 neutrons from βn (? in ^{137}Sb βn=49%) should be used for photo-ion current monitoring or/and background suppression

MR-TOF at ISOLDE

Multi-reflection time-of-flight mass separator (MR-TOF MS)

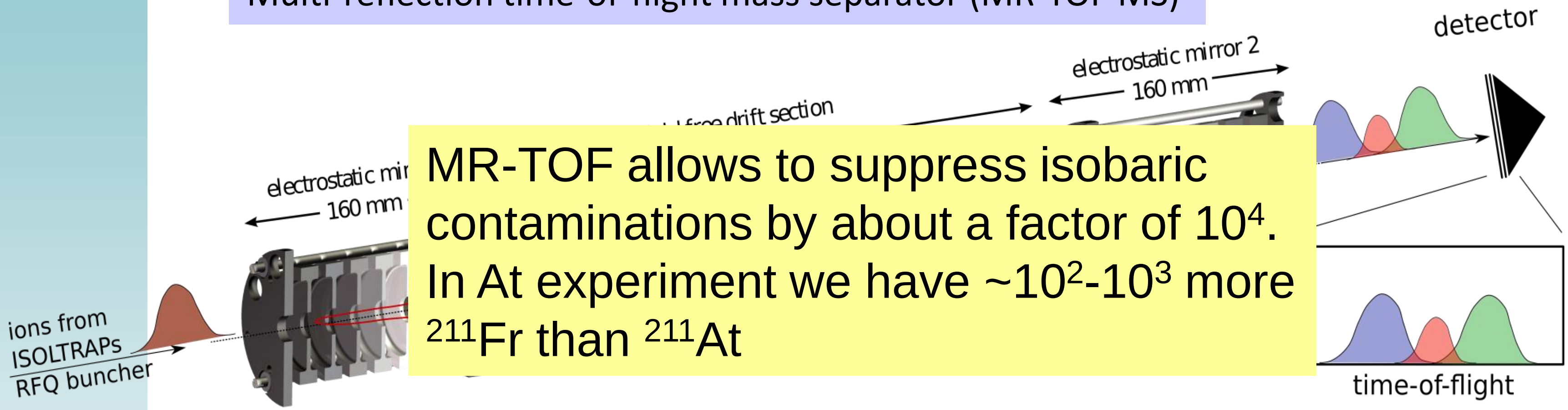

MR-TOF allows to suppress isobaric contaminations by about a factor of 10^4. In At experiment we have ~10^2-10^3 more ^{211}Fr than ^{211}At

Measurement of ^{82}Zn (MR-TOF+ISOLTRAP) was successful despite the isobaric contamination of ^{82}Rb being ***eight*** orders of magnitude more abundant (K. Blaum *et al,* Phys. Scr. T152 (2013) 014017)

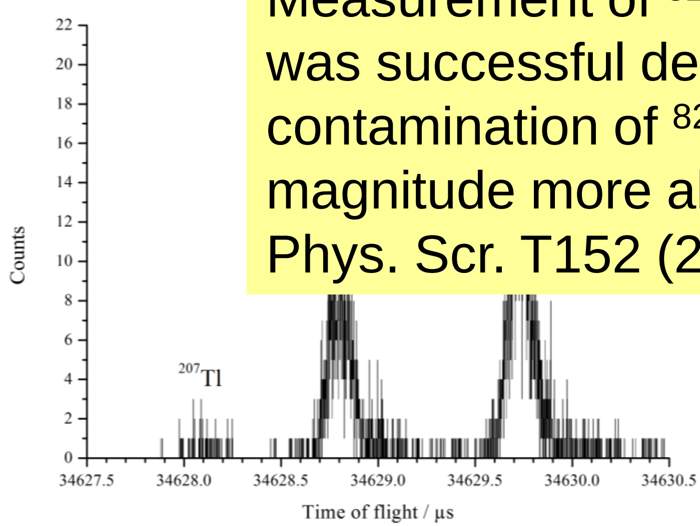

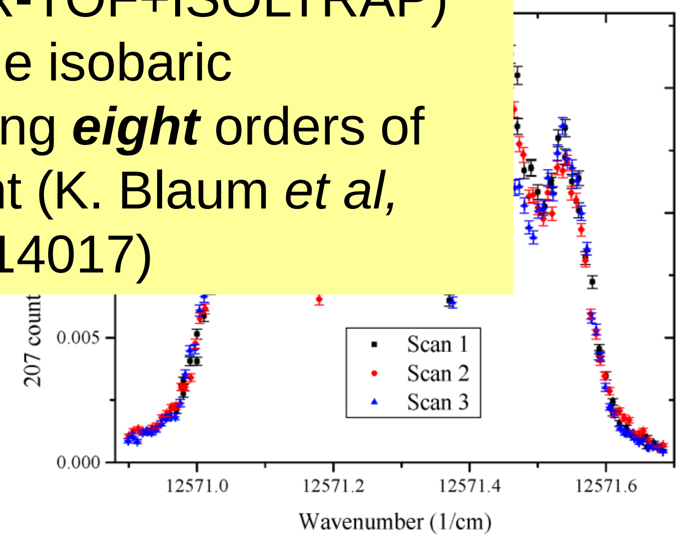

R. N. Wolf *et al*., Nucl. Instr. and Meth. A 686, 82-90 (2012), S. Kreim *et al.,* INTC-P-299, IS 518 (2011)

IRINA

1. Onset of deformation near N=60

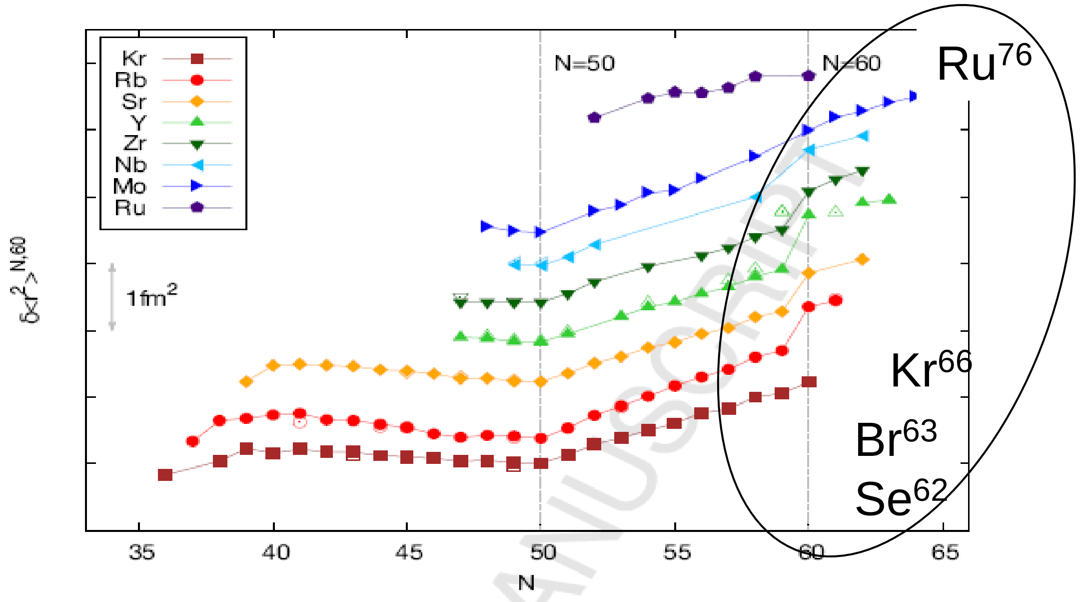

2. Octupole deformation at A~150 (Ba, Cs…)

3. Indium: high-spin isomers ($21/2^-$, $29/2^+$), anomalous behaviour of μ for $1/2^-$ isomer, shell-effect at N=82

Previously measured Achievable at IRINA

$^{104-127}In^{55-78}$ → up to N=87

4. … …

IRINA: conclusions and outlook

Рекордные выходы n-избыточных ядер в диапазоне от $_{25}$Mn до $_{68}$Er

1. Новая информация о $T_{1/2}$ и βn для моделирования r-процесса
2. Сосуществование форм в области 28<N<40, исчезновение подоболочки N=40
3. Уменьшение спаривания при N<82, сжатие оболочечной щели при N=82 и Z=28 (?), влияние 3N сил (?)
4. Исчезновение оболочечного эффекта в зарядовых радиусах при N=50 (Ni) и N=82 (Sn): насколько правильно описываются спин-орбитальные силы в RMF? Влияние перераспределения одночастичных состояний?
5. Одночастичные состояния вблизи N=50, Z=28: влияние тензорных сил (?)
6. Одночастичные состояния вблизи N=82, Z=50: влияние тензорных сил (?)
7. Новое магическое число N=90 (?)
8. Использование MR-TOF и ПИТРАП для уменьшения фона
9. Квадрупольная деформация при N>60, октупольная деформация вблизи A=150; классическая область деформации вблизи середины нейтронной оболочки (N=104); высокоспиновые изомеры в In … …

IRINA: In isotopes

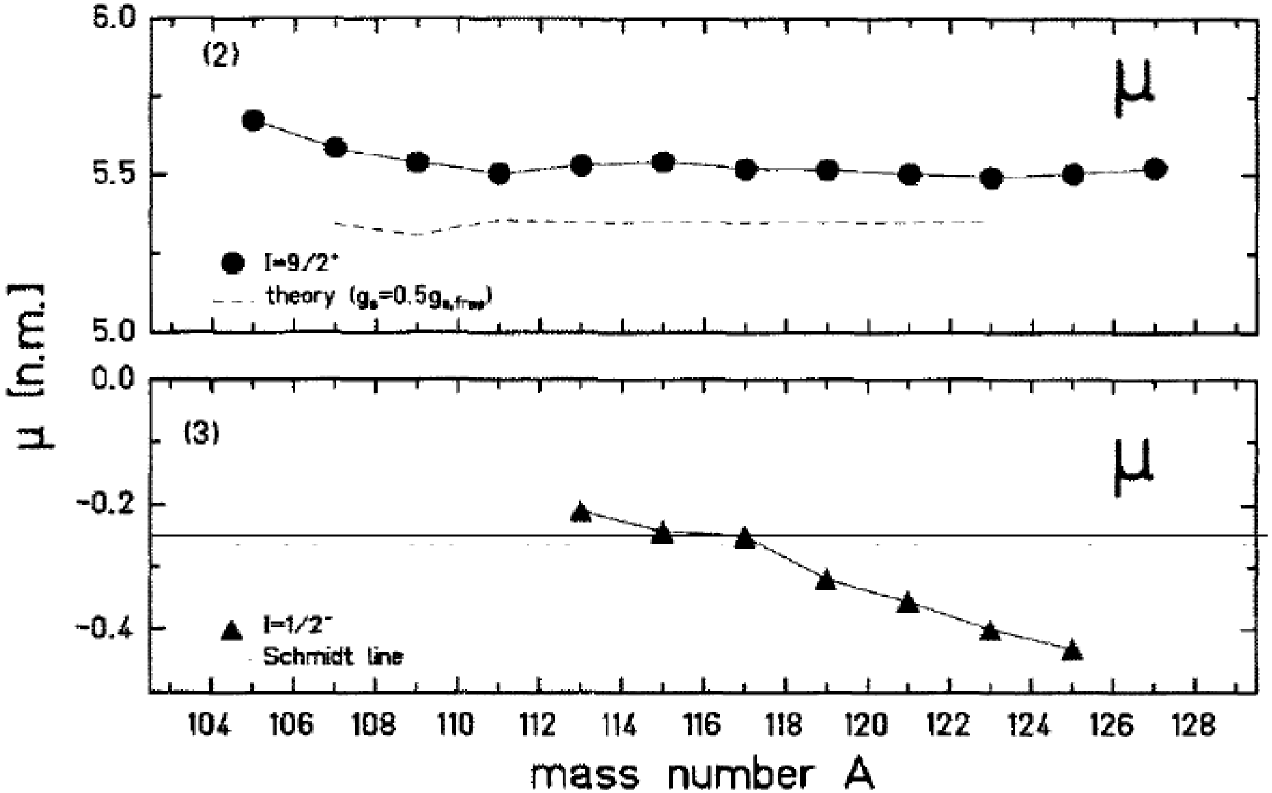

No μ for high-spin isomers ($21/2^-$, $29/2^+$)

IRINA: r-process

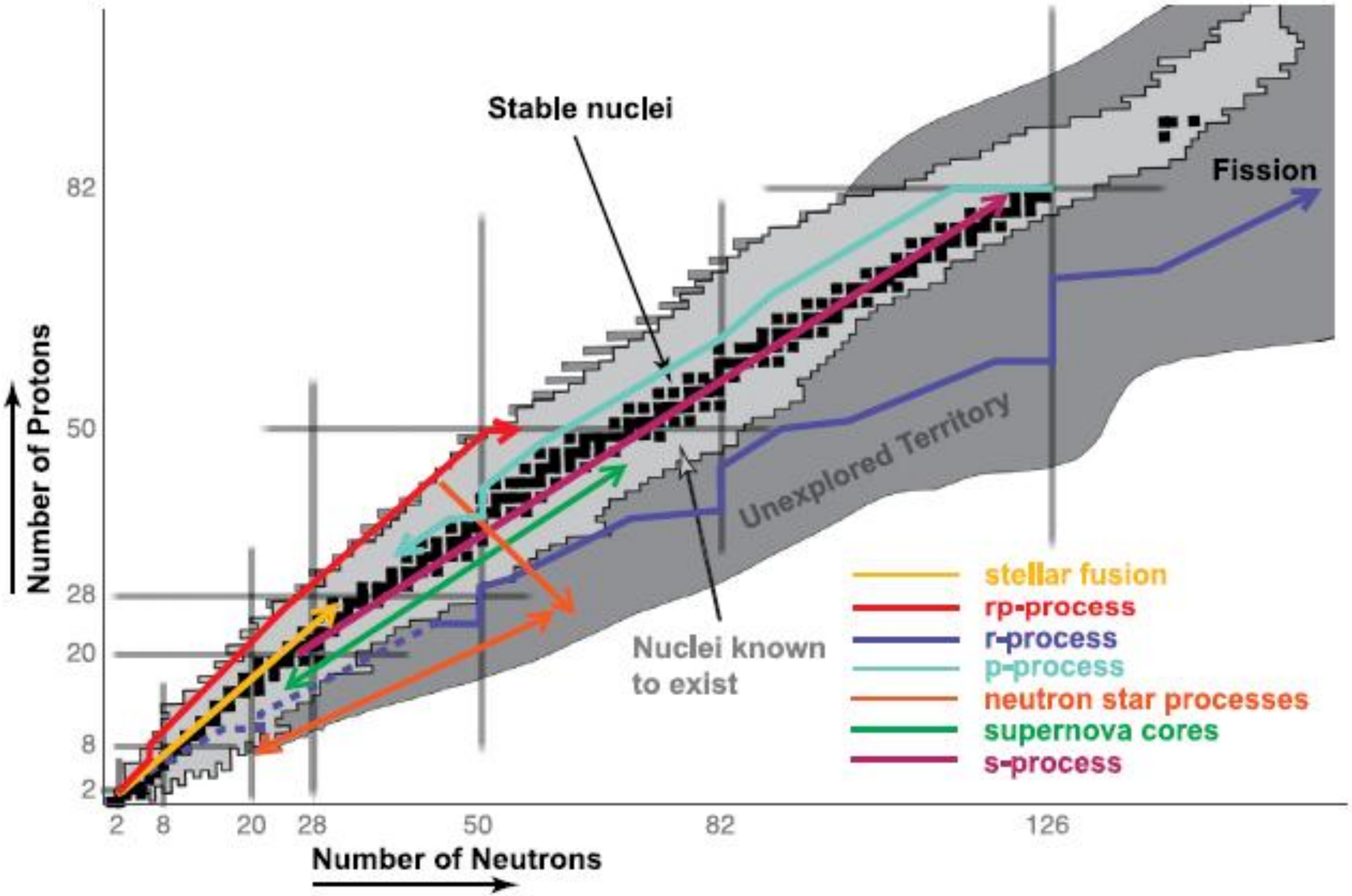

Schematic outline of the various nuclear reaction sequences in astrophysical environments on the chart of nuclides.